A&A manuscript no.
(will be inserted by hand later)

Your thesaurus codes are:
02.13.4; 02.13.5; 08.16.4; 08.03.1; 08.03.4; 08.13.2

ASTRONOMY
AND
ASTROPHYSICS
14.4.1997

MgO dust nucleation in M–Stars: Calculation of cluster properties and nucleation rates

T. M. Köhler[1,2], H.-P. Gail[2], E. Sedlmayr[1]

[1] Institut für Astronomie und Astrophysik, Technische Universität Berlin, Hardenbergstr. 36, 10623 Berlin, Germany
[2] Institut für Theoretische Astrophysik, Tiergartenstr. 15, 69121 Heidelberg, Germany

Received date ; accepted date

Abstract. The abundant metals Mg and Fe together with SiO form the iron-magnesium-silicate dust observed in the circumstellar shells of M-Stars. This dust component cannot nucleate directly from the gas phase but requires for its formation a different kind of seed nuclei. Further, there are some hints that besides the silicatic main dust component dust materials of a different composition may be present, perhaps oxides of iron and magnesium. We study in this paper the possibility that MgO particles are formed by nucleation from the gas phase and may form a dust component of their own or act as seed nuclei for the silicate dust.

For this purpose we calculated the structures and bond energies for small MgO clusters. The calculation is based on a modification of the classical Rittner potential model for alkali halide molecules and clusters. An additional parametrized attractive term is introduced to simulate a large covalent contribution to the bonding in II-VI compounds like MgO. We calculated cluster structures and bond energies with this empirical potential for cluster sizes N up to 16. Magic cluster sizes of enhanced stability are found for cluster sizes 2, 4, 6, 9, 12 and 15 for MgO. Their structure for $N \geq 6$ agrees well with experimental results and predictions from Hartree-Fock calculations.

The results for the cluster properties are used to calculate particle densities of $(MgO)_N$-clusters in stellar winds of late type giants and the rate of dust particle formation by nucleation of MgO. The nucleation rate of MgO turns out to be too small to form directly from the gas phase as a separate dust component or to form the seed nuclei for silicate dust formation.

Key words: Molecular data – Molecular processes – Stars: AGB and post-AGB – Stars: late-type – circumstellar matter – mass-loss

Send offprint requests to: H.-P. Gail

1. Introduction

Single stars with an initial mass of less than $\approx$ 8 solar masses arrive at the end of their life on the asymptotic giant branch (AGB). In this stage of their evolution they are cool supergiant stars with surface temperatures $\lesssim 3\,000$ K and their luminosities are typically of the order of $10^4\,L_\odot$ (Iben 1991). This last phase of stellar life is governed by strong mass loss which is accompanied and probably driven by dust condensation in the stellar wind. The formation of thick circumstellar dust shells makes such stars prominent emitters of infrared emission. Thousands of such objects have been detected by the IRAS satellite. They are the main sites of dust formation in space.

The unraveling of the basic microscopic processes responsible for the formation of dust in these circumstellar shells is still an unsolved problem. Despite much effort (for a review see E. Sedlmayr 1994) no definite conclusion has been arrived at for the basic processes working in the two different main types of cosmic dust making factories:

– the circumstellar shells around the M-stars with an oxygen rich element mixture which form some kind of iron-magnesium-silicate dust and
– the circumstellar shells around the C-stars with a carbon rich element mixture which form some kind of carbon dust, probably just ordinary soot.

The main obstacle to further progress is the lack of fundamental data on the basic chemical reactions in the gas phase and at the surfaces of growing clusters and on the properties of the particles involved in the process. The present state and the requirements for future laboratory research is described in Patzer et al. (1995). In this paper we attempt to study one possible process for the nucleation of dust in circumstellar shells around M-stars from the very beginning by calculating the basic properties of the clusters involved in the nucleation process and determining from this the nucleation rate.

The main dust component formed in M-star dust shells consists of some kind of amorphous silicate dust (for a discussion of its structure see Nuth and Hecht 1990) but this dust material cannot nucleate directly from the gas phase as particles with this composition and structure. Instead it requires for its formation the formation of some different kind of seed nuclei (e.g. Gail and Sedlmayr 1987). At first glance the most promising process for this seems to be first nucleating SiO and then growing the magnesium-silicate dust by surface reactions with Mg, Fe and SiO together with the abundant water vapour as an oxidizing agent. A model calculation for the stellar wind, however, indicated that this process yields a lower dust formation temperature than is generally derived from models for the IR-emission from circumstellar shells (Gail and Sedlmayr 1986) and, thus, a different process of formation of seed nuclei seems to be required in most cases. There are some indications of the existence of additional dust components in M-star shells (see the discussion in Henning et al. 1995) which may be pure magnesium-iron oxides. We explore in this paper the possibility that the direct nucleation of MgO from the gas phase occurs in circumstellar shells of M-stars which either forms MgO dust particles of their own or serve as seed nuclei for silicate dust formation.

For this purpose we calculated the properties of MgO using a semi-empirical potential model which extends the classical potential model used for calculating cluster structures of alkali halide ionic clusters to alkaline earth clusters which are not pure ion clusters but for which the bonding shows a marked covalent contribution. The structure of a $(MgO)_N$-cluster is calculated from the potential model and these results are used to calculate thermodynamic functions for the clusters and their equilibrium abundances. This enables us to determine the nucleation rate of MgO in circumstellar shells.

The plan of this paper is as follows. In sect. 2 we define the potential model for MgO, in sect. 3 we present the results of the calculations of the cluster structures, sect. 4 discusses the cluster size spectrum in a thermodynamic equilibrium state, sect. 5 shows how this can be used for calculating the nucleation rate. Section 6 gives our conclusions and the appendix gives a brief description of the method used for determining the minima of the potential hypersurface.

2. A semiempirical potential model for II-VI compounds

We shall calculate the structure and the properties of the MgO solid on the one hand and the structure and properties of the molecules MgO and their clusters $(MgO)_N$ on the other hand on the basis of a single, semi-empirical potential model, which is defined in this chapter.

2.1. Born–Mayer potential for ionic crystals

The magnesium oxide solid is believed to be a pure ionic compound formed from Mg^{++} cations and O^{--} anions, respectively. The crystal structure of the solid MgO according to X-ray diffraction studies is of the NaCl lattice type.

The bond properties and structures of ionic crystals can well be represented by the classical Born-Mayer (1932) potential model

$$\Phi = -\frac{1}{2}\sum_{\substack{i,j\\ i\neq j}} \frac{Z_i Z_j e^2}{r_{ij}} + \frac{1}{2}\sum_{\substack{i,j\\ i\neq j}} A_{ij}\mathrm{e}^{-\frac{r_{ij}}{\rho_{ij}}}\,, \tag{1}$$

representing the Coulomb interaction between the ions of charge Z_i (positive for the alkali cations and negative for the halogen anions in the case of I-VII compounds) at mutual distances r_{ij} and the repulsion due to overlap of the outer electron shell represented by the exponential term (Unsöld 1927). The distance ρ_{ij} measures the steepness of the repulsive part of the potential and A_{ij} its strength. Usually it is assumed that for a given compound the coefficients A_{ij} and ρ_{ij} are independent of the interacting particles i, j (but they are different for different substances). This potential and its consequences for the structure and properties of ionic crystals are discussed in detail in standard textbooks on solid state physics.

For a given crystal structure the summation for the Coulomb potential term can be done with the result

$$\Phi_{\mathrm{ch}} = -\frac{1}{2}\sum_{\substack{i,j\\ i\neq j}} \frac{Z_i Z_j e^2}{r_{ij}} = -M\frac{Z^2e^2}{r}N \tag{2}$$

for the contribution of the interaction between point charges to the total energy. M is the Madelung constant which equals $M = 1.747558\ldots$ for the NaCl lattice structure and N is the number of particles. The repulsive potential rapidly drops with increasing mutual distance r_{ij} of the particles. In a solid with NaCl lattice structure each ion is surrounded by 6 neighbours of the opposite charge at distance r, 12 ions of equal charge at distance $\sqrt{2}r$, 8 neighbours of opposite charge at distance $\sqrt{3}r$ and so on. For calculating the contribution of the repulsive potential to the total energy it suffices to consider the interaction with nearest neighbours only. The total repulsive energy in this approximation is

$$\Phi_{\mathrm{rep}} = 6A\mathrm{e}^{-\frac{r}{\rho}}N\,. \tag{3}$$

The total energy of a big macroscopic ionic crystal with NaCl structure is

$$\Phi = \left(-M\frac{Z^2e^2}{r} + 6A\mathrm{e}^{-\frac{r}{\rho}}\right)\cdot N\,. \tag{4}$$

Minimizing this with respect to the distance r between nearest neighbours yields for the equilibrium distance r_0 in the ionic lattice the equation

$$\mathrm{e}^{-\frac{r_0}{\rho}} = \frac{M}{6}\frac{Z^2e^2\rho}{Ar_0^2}\,. \tag{5}$$

r_0 can be determined from X-ray diffraction studies or from the relation

$$\rho_D = \frac{1}{2}\frac{m_+ + m_-}{r_0^3} \tag{6}$$

between the specific weight ρ_D of the solid, the masses m_-, m_+ of the anions and cations and the equilibrium distance in a lattice

Table 1. Calculated and experimental lattice energies of some oxides.

solid	$E_{L,\text{calc}}$ kJ mol^{-1}	$E_{L,\text{exp}}$ kJ mol^{-1}	solid	$E_{L,\text{calc}}$ kJ mol^{-1}	$E_{L,\text{exp}}$ kJ mol^{-1}
BeO	4293	4443	SrO	3217	3223
CaO	3414	3401	BaO	3029	3054
MgO	3795	3791			

Data from Weast et al. (1988)

of the NaCl type. The total lattice energy (per anion-cation pair) is obtained as

$$E_L = -M\frac{Z^2e^2}{r_0}\left(1-\frac{\rho}{r_0}\right) . \tag{7}$$

This energy may be obtained, for instance, from the well known Born-Haber cycle from the vapourisation energy of the solid and from the ionisation energy and electron affinity of the cation and anion, respectively.

The compressibility K_0 of the solid is

$$\frac{1}{K_0V} = \frac{\mathrm{d}^2\Phi}{\mathrm{d}V^2} \tag{8}$$

where $V = 2Nr^3$ denotes the volume. This yields the following relation at $r = r_0$

$$\frac{18r_0^4}{K_0MZ^2e^2} - 2 = \frac{r_0}{\rho} . \tag{9}$$

This together with Eq. (5) and the known equilibrium distance r_0 determines the unknown parameters A and ρ in the repulsive part of the Born–Mayer potential (4). An independent check of the validity of the model is the comparison of calculated lattice energies from (7) and experimental values from the Born–Haber cycle. The accuracy this model is satisfactory for the alkali halogenides (I–VII compounds) (compare the compilation of data in Weast et al. (1988), for instance) and it is applicable with sufficient accuracy to II–VI compounds like MgO (cf. Tab. 1).

2.2. The Rittner potential model for ion clusters

For small clusters and molecules the Born-Mayer potential model needs some modification. The ions do not only bear an electric charge but they are polarizable by the local electric field and then carry additionally higher electric multipole moments[1]. The induced electric multipole moments mutually interact and contribute to the total energy. For the highly symmetric, infinitely extended ionic crystals of cubic symmetry the local electric fields vanish at the equilibrium position of the ions, such that there is no net induced polarization of the ions and no contribution of this to the potential. For small particles of finite size there is no such high symmetry as viewed from the positions of the individual particles and therefore, there exists a local electric field which polarizes the ion. Rittner (1951) introduced such additional terms in order to discuss the properties of diatomic alkali-halide molecules. The dominating contributions to the potential energy are the monopole—induced dipole interaction, the induced-dipole–induced-dipole interaction and the work required to form the induced dipole moment. It has been shown (O'Konski 1955) that these contributions can be rearranged into the form

$$\Phi_{\text{ind}} = -\frac{1}{2}\sum_{\substack{i,j\\ i\neq j}}\frac{Z_ie\left(\boldsymbol{\mu}_j\cdot\boldsymbol{r}_{ij}\right)}{r_{ij}^3} , \tag{10}$$

where

$$\boldsymbol{\mu}_j = \alpha_j\boldsymbol{E}_j = \alpha_j\sum_{\substack{k\\ k\neq j}}\left[\frac{Z_ke\boldsymbol{r}_{kj}}{r_{kj}^3} + \frac{3\boldsymbol{r}_{jk}(\boldsymbol{\mu}_k\cdot\boldsymbol{r}_{jk})}{r_{jk}^5} - \frac{\boldsymbol{\mu}_k}{r_{j,k}}\right] \tag{11}$$

is the induced dipole moment due to the local electric field $\boldsymbol{E}$ of all charges Z_k and induced dipoles μ_k at the position of particle j. α_j is the polarizability of the j-th particle. This potential was first applied by Rittner (1951) to calculate the properties of diatomic alkali halides and by O'Konski and Higuchi (1955) and by Berkowitz (1958, 1958) for calculating the properties of the dimers. Martin (1983) applied this model to the calculation of NaCl clusters. Brumer and Karplus (1973) derived potential energy terms from second order perturbation theory and identified these terms with the Rittner potential model.

Additionally the van der Waals attraction potential contributes to the potential energy. This usually yields a correction of less than one percent to the total bond energy originating from the electrostatic forces and is neglected in the present calculation.

For the diatomic ionic molecules the potential may be written as

$$\begin{aligned}\Phi(r) \;=\; & A\mathrm{e}^{-\frac{r}{\rho}} - \frac{Z^2e^2}{r} - \frac{Ze\mu_1}{r^2} - \frac{Ze\mu_2}{r^2} \\ & -\frac{2\mu_1\mu_2}{r^3} + \frac{\mu_1^2}{2\alpha_1} + \frac{\mu_2^2}{2\alpha_2}\end{aligned} \tag{12}$$

The second row describes the dipole-dipole interaction and the work required to form the induced dipoles if the two ions approach each other from infinity. The induced dipole moments μ_i are

$$\mu_i = \frac{r^4Ze\alpha_i + 2rZe\alpha_1\alpha_2}{r^6 - 4\alpha_1\alpha_2} . \tag{13}$$

Usually for ionic molecules one has polarizabilities of the order of $\alpha_- \approx 2\,\text{Å}^3$, $\alpha_+ \approx 0.5\,\text{Å}^3$ and distances r of the order of $r \approx 1.5\,\text{Å}$. Then $r^6 \gg 4\alpha_1\alpha_2$ and one may develop the rhs. of (13) into a series

$$\mu_i = \frac{Ze\alpha_i}{r^2} + \frac{2Ze\alpha_1\alpha_2}{r^5} + \frac{4Ze\alpha_i\alpha_1\alpha_2}{r^8} + \cdots \tag{14}$$

[1] We do not consider particles which carry *permanent* electric dipole and higher multipole moments.

Table 2. Properties of MgO. The formation energy ΔH_f of the solid is that from free atoms. κ is the compressibility

	Solid	Source		Source
Mol. wt.	40.31	a		
ρ_D [g/cm^3]	3.58	a		
r_e [nm]	0.211	b		
ΔH_f[kcal mol^{-1}]	-236.6	a		
κ[cm^2/dyn]	6.01 10^{-13}	f		
	Molecule			
r_0 [nm]	0.1749	c		
μ[AMU]	9.5958	c		
D_0 [eV]	-3.47	g		
ω_e[cm^{-1}]	785.06	c		
	Ions			
	Mg^+		Mg^{++}	
I[eV]	7.646	a	15.035	a
$\alpha[10^{-24}$cm^3]			0.094	d
	O^-		O^{--}	
E_{el}[eV]	-1.461	a, e	6.41	a
$\alpha[10^{-24}$cm^3]			1.685	h

Sources:
a) Weast et al. 1988 e) Branscomb 1962
b) Pauling 1960 f) Sumino et al. 1983
c) Huber & Herzberg 1979 g) JANAF Tables, Chase et al. 1985
d) Landolt-Börnstein 1981 h) Fowler and Maddon 1985

Keeping terms up to the second order from this series results in the following potential for the diatomic molecule

$$\Phi(r) = A\mathrm{e}^{-\frac{r}{\rho}} - \frac{Z^2e^2}{r} - \frac{Z^2e^2(\alpha_1+\alpha_2)}{2r^4} - \frac{2Z^2e^2\alpha_1\alpha_2}{r^7} \,. \quad (15)$$

If one compares this model with the results of quantum mechanical perturbation calculations, it turns out that the model corresponds to the perturbation theoretical result up to the second order, except for the term $\propto r^{-7}$ which is of third order (Brumer and Karplus 1973). For consistency this term is neglected. Brumer and Karplus call this special potential model the T(runcated)-Rittner-Potential.

The potential model depends on the two free parameters A and ρ which can be determined from experimentally determined properties of the molecule, for instance from its bond length and bond energy. For alkali halide compounds, usually the results for the molecule and the solid agree satisfactorily (cf. Martin 1983) and the potential model then can be applied to calculate cluster properties for the whole size regime between the molecule and the macroscopic solid.

2.3. Extension of the T-Rittner potential model

This T-Rittner potential model has been applied by Zieman and Castleman (1991) to model small alkaline–earth clusters, but with unsatisfactory results. It turns out that the parameters A and ρ as determined from the solid and the molecule, respectively, do not agree to within reasonable limits. The reason for the discrepancy can be traced back to the charge carried by the ions:

– For the solid II-VI compounds the two different ions carry a charge equal to two elementary charges. Causa et al. (1986) give a value of $Z = \pm 1.95$ for MgO.
– The effective charge of the atoms in the diatomic molecule on the other hand is much less. Zieman and Castleman (1991) and Recio et al. (1993) found from ab initio calculations an effective charge of the O and Mg in MgO of $Z = \pm 0.81$.

That this difference in the effective charge carried by the ions in the molecule and the solid, respectively, is real can be seen from the fact that the properties of the diatomic molecule can be fit much better with a T-Rittner potential if an effective charge of $Z_{\rm eff} = \pm 1$ is used (Zieman and Castleman 1991).

On the molecular level, the bonding of the II-VI compounds is not (more or less) purely ionic as it is in the case of I-VII compounds but it has a pronounced covalent contribution. The moderate difference of the electronegativity of such compounds also points to a considerable contribution of covalent bonding (Pauling 1960). This covalent contribution, however, disappears in the solid where the bonding for the alkaline earth compounds is of (nearly) purely ionic character.

The potential of covalently bound diatomic molecules usually can be modeled with sufficient accuracy by the well known Morse potential

$$\Phi_M(r) = D_0\left(\mathrm{e}^{-2ax} - 2\mathrm{e}^{-ax}\right) \quad \text{with} \quad x = \frac{r-r_0}{r_0}\,, \quad (16)$$

where r_0 denotes the equilibrium distance of the atoms and D_0 is the depth of the potential which equals its dissociation energy reduced by the contribution of the zero-point energy of the vibrations. a is a free parameter, which usually is fitted by requiring

$$\mu\omega^2 = \left.\frac{\mathrm{d}^2\Phi(r)}{\mathrm{d}r^2}\right|_{r=r_0} = 2D_0\left(\frac{a}{r_0}\right)^2 \,. \quad (17)$$

μ is the reduced mass and ω the vibrational frequency of the molecule. The Morse potential may be written as

$$\Phi_M(r) = A\mathrm{e}^{-2\frac{r}{\rho}} - B\mathrm{e}^{-\frac{r}{\rho}} \quad (18)$$

with

$$A = D_0\mathrm{e}^{2a}\,,\ B = 2D_0\mathrm{e}^{a}\,,\ \rho = \frac{r_0}{a}$$

which shows a repulsive term similar to the corresponding term in the Born-Mayer potential and an exponential attractive term characteristic of the covalent bonding.

The transition between the two types of bonding, the mixed ionic and covalent bonding for the diatomic molecule and the pure ionic bonding in the solid, must occur somewhere in the size region of clusters. Parallel to the change in bonding character the effective charge carried by the ions must increase from its value $Z_{\rm eff} \lesssim 1$ for the diatomic molecule to $Z_{\rm eff} \approx 2$ for the solid. This suggests merging both potential models, the T-Rittner potential (15) on the one hand and the Morse potential (18) on the other hand, into a combined model to obtain a potential model for the whole size regime between molecules and solids

$$\Phi(r) = A\mathrm{e}^{-\frac{2r}{\rho}} - B\mathrm{e}^{-\frac{r}{\rho}} - \frac{Z_{\rm eff}^2 e^2}{r} - \frac{Z_{\rm eff}^2 e^2(\alpha_1+\alpha_2)}{2r^4} \,. \tag{19}$$

The quantity B describes the covalent attraction. It vanishes in the solid state since there the bonding character is purely ionic, but for small clusters it is nonzero. Hence B depends on the cluster size N (N=number of monomers forming the cluster). The same holds for the effective charge $Z_{\rm eff}$ on the ions which changes from ± 1 to ± 2. Since presently there is no evidence to indicate how both quantities vary with cluster size we decided to use the following simple interpolation formula

$$Z_{\rm eff}(N) = \pm\frac{2\zeta N+1}{\zeta N+1} \,. \tag{20}$$

With $\zeta \ll 1$ this changes from slightly more than $Z_{\rm eff} = \pm 1$ for $N = 1$ to $Z_{\rm eff} = 2$ in the limit $N \to \infty$. ζ may be used to adapt the cluster size region where the transition between the two limit cases is assumed to occur. We choose in our calculation $\zeta = 1/20$ which results in $Z_{\rm eff} = \pm 3/2$ at a cluster size $N = 20$, i.e. we essentially use the small cluster limit $Z_{\rm eff} \approx \pm 1$ for all small clusters which may be of relevance for a possible condensation process. The term B is interpolated in the calculations as follows

$$B(N) = B_1(2 - |Z_{\rm eff}|)^2 \,. \tag{21}$$

B is assumed to contribute only to the interaction potential between the cations and anions since it seems plausible that only these can share to some extent their electrons resulting in a covalent bonding.

The potential of a cluster of size N now is

$$\Phi(N) = \sum_{\substack{i,j\\ i>j}} A\,\mathrm{e}^{-\frac{2r_{ij}}{\rho}} - \sum_{\substack{i,j\\ i>j}} B(N)\,\mathrm{e}^{-\frac{r_{ij}}{\rho}} - \sum_{\substack{i,j\\ i>j}} \frac{Z_{{\rm eff},i} Z_{{\rm eff},j} e^2}{r_{ij}} - \frac{1}{2}\sum_{\substack{i,j\\ i>j}} \frac{Z_{{\rm eff},i} e\, \boldsymbol{\mu}_j \cdot \boldsymbol{r}_{ij}}{r_{ij}^3} \tag{22}$$

where

$$\boldsymbol{\mu}_j = \alpha_j \sum_{\substack{k\\ k\neq j}} \frac{Z_{{\rm eff},jk} e\, \boldsymbol{r}_{kj}}{r_{kj}^3} \tag{23}$$

is the induced dipole moment on particle j.

Table 3. Fit of the potential model for MgO

	Parameters for MgO		
A	$1.61799\ 10^{-9}$	erg	
B_1	$1.06680\ 10^{-10}$	erg	
ρ	$6.42223\ 10^{-9}$	cm	
Properties	calculated	measured	error %
D_0[kcal/mol]	-156.60	-156.60	fit
r_0(mol)[cm]	$1.693\ 10^{-8}$	$1.749\ 10^{-8}$	-3.2
ω[cm^{-1}]	785.0	785.0	fit
$\mu_{\rm Dip}$[Debye]	4.845	6.26	-22.6
$E_{\rm lattice}$[kcal/mol]	-907.40	-907.40	fit
r_0(lattice)[cm]	$2.182\ 10^{-8}$	$2.11\ 10^{-8}$	3.9
κ[cm^2/dyn]	$5.273\ ^{-13}$	$6.01\ 10^{-13}$	12.3

2.4. Fitting the parameters

The three free parameters A, ρ and B_1 of the potential model (22) can be determined by fitting these coefficients such that some of the observed quantities of the diatomic molecule and the bulk solid are reproduced. A comparison of additional measured quantities for both substances with predictions for its value from the potential model serve as a test of the reliability and accuracy of the potential model.

For the potential (19) we obtain for the dissociation energy of the diatomic molecule

$$D = A\mathrm{e}^{-\frac{2r_0}{\rho}} - B\mathrm{e}^{-\frac{r_0}{\rho}} - \frac{Z_{\rm eff}^2 e^2}{r_0} - \frac{Z_{\rm eff}^2 e^2(\alpha_1+\alpha_2)}{2r_0^4} \tag{24}$$

with r_0 being the equilibrium distance of the two atoms. r_0 follows from $\Phi' = 0$ which yields the equation

$$2A\mathrm{e}^{-\frac{2r_0}{\rho}} - B\mathrm{e}^{-\frac{r_0}{\rho}} - \frac{\rho}{r_0}\left[\frac{Z_{\rm eff}^2 e^2}{r_0} + 2\frac{Z_{\rm eff}^2 e^2(\alpha_1+\alpha_2)}{r_0^4}\right] = 0 \,. \tag{25}$$

The vibrational frequency ω of the molecule follows from the equation of motion in the harmonic oscillator approximation (17) as

$$\rho^2\mu\omega^2 = 4A\mathrm{e}^{-\frac{2r_0}{\rho}} - B\mathrm{e}^{-\frac{r_0}{\rho}} - \frac{\rho^2}{r_0^2}\left[\frac{2Z_{\rm eff}^2 e^2}{r_0} + \frac{10 Z_{\rm eff}^2 e^2(\alpha_1+\alpha_2)}{r_0^4}\right] \,. \tag{26}$$

For the solid on the other hand the potential (22) reduces to the limiting case of the standard Born-Mayer potential (4)

$$\Phi_{\rm sol}(r) = 6A\mathrm{e}^{-\frac{2r}{\rho}} - \frac{M Z_{\rm eff}^2 e^2}{r}$$

The crystal lattice energy is

$$U_{\rm Coul} = 6A\mathrm{e}^{-\frac{2r_{\rm e}}{\rho}} - \frac{M Z_{\rm eff}^2 e^2}{r_{\rm e}} \tag{27}$$

Table 4. Calculated properties of MgO-clusters: Potential $\Phi(N)$, bond energy per monomer $\Delta E_0(N)/N$, the three principal moments of inertia I and the symmetry number σ

N	$\Phi(N)$ eV	$\Delta E_0/N$ eV	I_x	I_y 10^{-38} g cm^2	I_z	σ
1	9.652		0.459	0.459	0.000	1
2	25.895	2.41	1.154	1.178	2.332	4
3(a)	41.978	3.00	2.347	3.809	5.250	6
3(b)	41.996	3.02	3.183	3.183	6.367	12
4(a)	62.105	4.07	5.155	5.155	5.155	1
4(b)	58.840	3.27	3.152	9.000	10.834	1
5(a)	79.770	4.06	6.700	9.148	10.729	1
5(b)	76.657	3.44	4.062	17.192	19.441	1
5(c)	80.137	4.12	7.310	7.310	9.917	4
6(a)	100.156	4.35	8.106	14.552	14.730	4
6(b)	95.285	3.55	4.930	29.513	32.246	1
6(c)	100.630	4.42	10.926	10.926	13.501	6
6(d)	100.344	4.38	9.227	12.599	13.738	1
7(a)	121.165	4.52	12.066	17.761	17.761	1
7(b)	120.219	4.40	14.142	14.387	18.370	1
8(a)	141.263	4.46	10.770	33.399	33.399	4
8(b)	143.066	4.67	16.304	21.185	21.753	1
8(c)	143.040	4.67	15.836	22.485	22.485	4
9(a)	164.130	4.61	14.915	34.631	35.200	1
9(b)	166.279	4.84	20.291	26.310	26.310	6
10(a)	185.349	4.51	13.495	64.081	64.188	4
10(b)	186.746	4.64	21.749	36.416	39.991	2
10(c)	189.303	4.89	27.144	27.608	32.334	1
11	212.807	4.91	23.882	43.308	44.394	1
12(a)	238.598	5.07	25.658	55.423	55.423	6
12(b)	240.317	5.20	36.073	38.569	41.555	1
13(a)	265.907	5.27	38.190	46.617	49.812	1
13(b)	264.210	5.14	44.019	44.174	48.362	1
14(a)	291.926	5.31	41.392	51.573	65.263	1
14(b)	294.640	5.49	40.320	50.668	57.684	1
15(a)	325.897	5.82	46.148	56.127	56.127	6
15(b)	317.582	5.28	30.792	101.786	101.786	6
16	348.930	5.58	56.928	62.732	68.059	1

where r_e is the equilibrium distance in the lattice which follows from

$$\Phi'_{sol} = 0 = -\frac{12A}{\rho} e^{-\frac{2r_e}{\rho}} + \frac{MZ_{eff}^2 e^2}{r_e^2} \tag{28}$$

We determined the parameters of our model by fitting three measured quantities of the diatomic molecule and the solid exactly. Other procedures are also possible, for instance least square fittings of more than three measured properties. For the calculation of thermodynamical data for the clusters the ground state energy needs the highest accuracy of all calculated data. Thus we decided to fit our model to the following set of measured properties:

- The bond energy of the molecule
- The vibrational frequency of the molecule
- The crystal lattice energy.

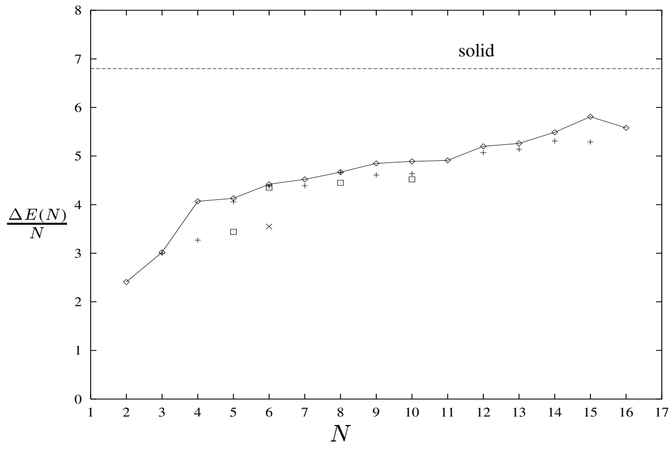

Fig. 1. Bond energy per monomer $\Delta E_0(N)/N$ in eV for MgO clusters of size N. The full line connects the ground state bond energies. The dotted line shows the bond energy of a monomer within the infinite solid. Other points correspond to less strongly bound structural isomers

Thus, we solved Eqs. (24), (26) and (27) for the parameters A, B and ρ. The resulting values of the potential parameters for MgO using the data from Tab. 2 are shown in Tab. 3. They need some comments:

1.) The parameters of the solid are rather uncritical. The lattice energy follows from the Born-Haber cycle as $U_{Coul} = -907$ kcal/mol. We used a value for the electron affinity for O^{--} of +6.41 eV for the solid which reproduces the lattice energy of alkaline earth oxides as given in the table in Weast et al. (1988).

2.) The value of the bond energy D_0 for the MgO is rather uncertain. Values between 2.3 eV and 4.3 eV have been reported. The lowest experimentally derived value is $D_0 = 2.6$ eV (Operti et al. 1989). Most experimentally determined values up to 1985 are listed in the JANAF table (Chase et al. 1985). They favour a value of $D_0 = 3.47$ eV which is the value for D_0 which we are using in our calculations. A similar value of $D_0 = 3.73$ eV is favoured in the J. Chem. Ref. Data (Pedley and Marshall 1983). Theoretical calculations for the MgO molecule have been performed by Bauschlicher et al. (1982, 1993) and Cuesta et al. (1991, 1993). The results for *ab initio* calculations tend to be lower than experimental values but it is by no means certain that these lower values are more realistic.

The bond energy of the MgO molecule with respect to formation from the free ions follows from the dissociation energy D_0 of the molecule, the ionisation energy I_{Mg} of the Mg atom, and the electron affinity E_O of the oxygen atom as

$$\Phi(r_0) = D_0 + I_{Mg} + E_O = -9.652 \text{ eV}. \tag{29}$$

This number is used for calculating formation energies of clusters from monomers.

3.) The polarizability of the free doubly charged negative oxygen ion O^{--} of $\alpha = 3.84 \cdot 10^{-24}\,\mathrm{cm}^3$ (Landolt-Börnstein 1981) does not allow for a reasonable potential fit. Usually within a compound the polarizability of a particle is less than that for the free particle and we therefore used in our calculations the polarizability of $\alpha = 1.685 \cdot 10^{-24}\,\mathrm{cm}^3$ which is obtained from the Clausius-Mosotti relation for the solid (Fowler and Madden 1985).

4.) A comparison of some calculated and measured values for MgO is given in Tab. 3. The match between measured properties of the diatomic molecule and the solid and that of the corresponding quantities calculated from the potential model is as good as can be expected for such calculations and can be considered satisfactory, though our model for II-VI compounds is not as accurate as the corresponding model for pure ionic I-VII compounds (e.g. Martin 1983).

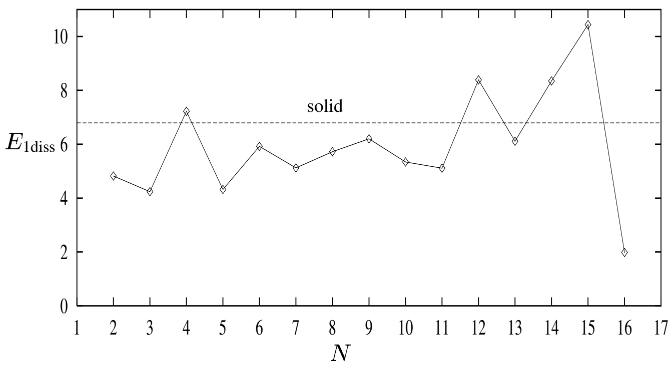

Fig. 2. Energy in eV required to dissociate a monomer from a cluster of MgO of size N. The dotted line corresponds to the bond energy of 6.8 eV of a monomer within the infinite solid

3. Cluster structure and properties

3.1. Calculation of the cluster potential

Any stable equilibrium configuration of a cluster with N monomers corresponds to a local minimum of the potential $\Phi(q_{i\mu})$ in the $6N$-dimensional space of the positions $q_{i\mu}$ of its individual atoms. In a system of many particles there exist numerous possible equilibrium configurations with different geometrical arrangements of the atoms and rather different binding energies. Usually most of the potential minima are rather shallow and do not really correspond to observable equilibrium structures of a cluster, but a few of them are quite deep. The deepest of all of these potential minima corresponds to the ground state configuration of the cluster and its depth to the dissociation energy of the ground state into the free ions. Other deep local minima correspond to stable isomers of the cluster and their depth to their dissociation energies, which are usually comparable to but (by definition) less than that of the ground state.

The basic problem in determining the structure and bond energy of a cluster then consists in finding the absolute minimum of the cluster potential $\Phi(q_{i\mu})$ and all other deep local potential minima with comparable depth to that of the absolute minimum. This corresponds to the notoriously difficult problem of optimising a nonlinear quality function. In the present calculation the task of determining the minima of the potential Φ was solved by applying the evolution strategy of Rechenberg (1973, 1989) which is described in the appendix. We determined by this method the minimum of the potential $\Phi(N)$ for all clusters of size up to $N = 16$. Further we determined all local energy minima, within a few eV away from the ground state, if such exist, which correspond to the stable isomers.

For each equilibrium configuration, the vibrational frequencies for the cluster can be calculated in the approximation of small vibrations from the eigenvalues of the force matrix. The results will be published elsewhere (Koehler et al. 1996).

3.2. Results for MgO clusters

The results of a calculation for the potential and structure of MgO clusters are shown in Tab. 4 and Fig. 3, respectively. The calculations were done for clusters consisting of up to 16 monomers. For each cluster size many runs of the optimizing procedure with different initial configurations have been carried out to be sure that we have found the true energy minimum representing the ground state configuration of a cluster of size N and all strong local minima within a few eV above the ground state, which represent isomeric structures of the N-cluster. For nearly all cluster sizes there exist some isomers with a bond energy per monomer nearly equal to that of the ground state.

The bond energy per monomer $\Delta E_0(N)/N$ is shown in Fig. 1. This bond energy is determined by considering that the ionisation energy and electron affinity of the cations and anions in the cluster are different from that in the monomer. The electron affinity $E_{\mathrm{el}}(N)$ of the fractionally charged anions in the clusters is determined by linear interpolation according to Z_{eff} between its values for the two limit cases $Z = 1$ and $Z = 2$ (given in Tab. 2). The ionization energy for the fractionally charged Mg-cations in the clusters is calculated according to the effective charge Z_{eff} and from the standard formula for the ionisation of hydrogen like ions

$$E_{\mathrm{ion}} = \frac{Rhc}{n^2}\, Z_{\mathrm{ion}}^2 Z_{\mathrm{e}}^2\,. \tag{30}$$

E_{ion} is the ionisation energy from a state with principal quantum number n, R is the Rydberg constant, and Z_{ion} and Z_{e} are the charges of the ion and the electron in units of the elementary charge, respectively. The effective charge of the Mg^{++} core is found from (30) and the ionisation energy of 15.035 eV required to remove the second 3s-electron from the free ion Mg^{+} to be $Z_{\mathrm{ion}} = 3.154$. We apply Eq. (30) to calculate the ionisation energy of a fractionally charged Mg cation with an effective charge $Z_{\mathrm{eff}} - 1$ of the electron located partially on the cation

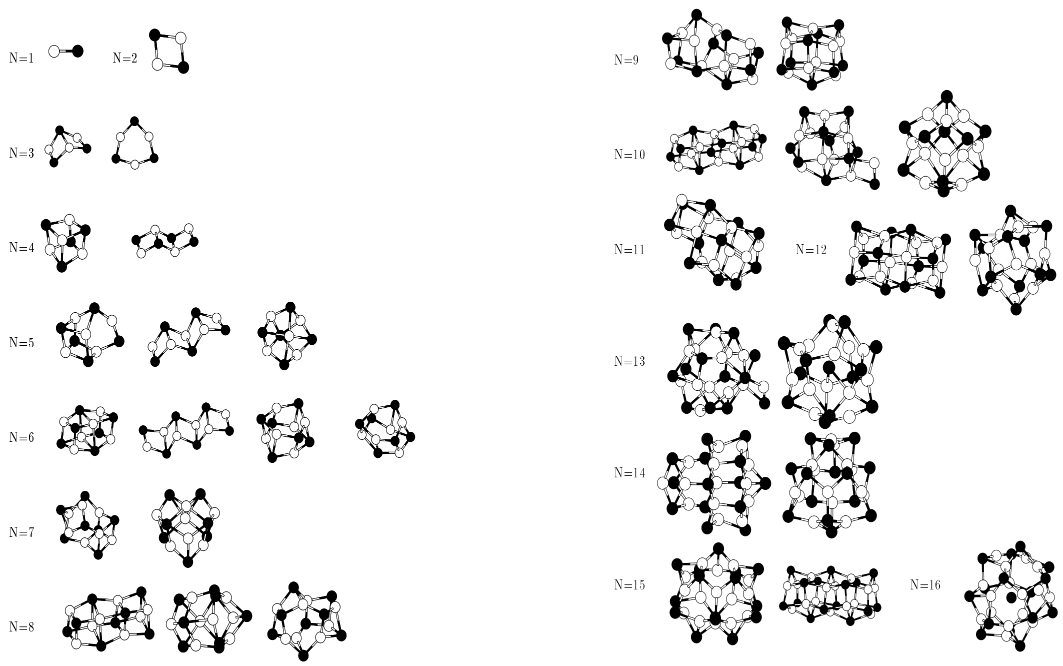

Fig. 3. Structures of MgO-clusters of size $N = 1, \ldots, N = 16$. White balls correspond to magnesium cations, black balls to oxygen anions.

with Z_{eff} given by (20). Then we calculate the ionisation energy as

$$I_N = \frac{Rhc}{n^2}\, Z_{\text{nuc}}^2\, (Z_{\text{eff}} - 1)^2\ . \tag{31}$$

The energy of formation $\Delta E_0(N)$ of a cluster of size N from the free monomers, finally, is obtained from the energy required to form the free ions from the fractionally charged particles bound in the cluster and the energy gain by recombining the free ions into the monomers as

$$\Delta E_0(N) = \Phi_N - N \cdot I_N + N \cdot E_{\text{el}}(N) - N \cdot \Phi_0\ . \tag{32}$$

Φ_0 is the energy of formation of the monomer from the free ions Mg^+ and O^- as given by (29).

The resulting bond energy $\Delta E_0(N)/N$ per monomer in the cluster is given in Tab. 4 and is shown in Fig. 1. For small cluster sizes N the average bond energy per monomer is much smaller than the bond energy of 6.79 eV of a monomer in the crystal lattice of the solid MgO. It increases with cluster size N and for the clusters with 15 and 16 monomers it is already only one eV below its bulk value. This behaviour is just what one would expect, that is that the bond energy of the monomers in the clusters increases more or less monotonically with increasing cluster size, but remains always less than in the solid.

Fig. 2 shows the energy

$$E_{1\,\text{diss}} = -(E_0(N) - E_0(N-1)) \tag{33}$$

required to dissociate the most stable cluster formed from N monomers into a cluster consisting of $N - 1$ monomers and into a free MgO molecule in the gas phase. The dependence of this dissociation energy on N shows clearly that clusters of size N = 2, 4, 6, 9, 12 and 15 show enhanced stability compared to clusters of size $N \pm 1$(magic numbers). This fits well to the findings from mass spectrometry experiments (Ziemann and Castleman 1991, Saunders 1988, 1989) and the results from Hartree-Fock calculations (Rezio et al. 1993).

The structures of the magic clusters are stacked hexagonal rings for $N > 4$, see Fig. 3, and only for the cluster with $N = 4$ shows the cubic structure of the solid. For $N = 2$ the structure is a rhomboid. There is a slight asymmetry in the bond angles between O-Mg-O and Mg-O-Mg which results from the different polarizabilities. The energy of the induced dipole moments strengthens the bond energy which is responsible for a tendency of the ions to arrange in such a way that the induced dipole moments are as large as possible, with the restriction, however, that equally charged ions should not come too close. This favours smaller bond angles at the particle with the higher polarizability, i.e. at the oxygen ion. Only for two clusters a plane structure is found: for the dimer $N = 2$ and for the ring with $N = 3$. The linear double chains with $N = 3, \ldots, 6$ are warped. The big clusters $10c$, $11a$ $12a, b$, $13a, b$, $14a, b$, $15a$ and 16 are cage molecules, their structure is probably determined by the high polarizability of the oxygen.

4. Thermodynamic properties of the MgO clusters

4.1. Calculation of the free enthalpy

The thermochemical properties of the MgO molecule and of its clusters $(MgO)_N$ can be determined once the enthalpy of formation ΔH_f of the clusters and their entropy is known. The enthalpy of formation of a cluster of N molecules from the corresponding free molecules is

$$\Delta H_f = \Delta E_0(N) + U(N,T) + RT \tag{34}$$

where $\Delta E_0(N)$ is given in Tab. (4) and $U(N,T)$ is the heat content of the internal degrees of freedom of the cluster.

The contribution of the vibrational degrees of freedom to the internal energy U of the cluster is

$$U_{\text{vib}}(N,T) = N_0 \sum_{\alpha=1}^{6N-6} \frac{h\nu_\alpha}{1 - \mathrm{e}^{-\frac{h\nu_\alpha}{kT}}} \tag{35}$$

with N_0 being the Avogadro number (note that N denotes the number of monomers, which are already diatomic). This is calculated using frequencies ν_α calculated in the approximation of small vibrations from eigenvalues of the force-matrix.

The translational, rotational, vibrational and electronic contributions to the partition function of a cluster are assumed to be independent of each other. The entropy in this case is additive in these contributions and we have

$$S_{\text{tr}} = 37.0 + \frac{3}{2} R \ln\left(\frac{40}{M}\right) + \frac{3}{2} R \ln\left(\frac{T}{298}\right) \tag{36}$$

for the contribution of the translational degrees of freedom,

$$S_{\text{rot}} = 6.9 + R \ln\left(\frac{I_x}{\sigma}\right) + R \ln\left(\frac{T}{298}\right) \tag{37}$$

for the contribution of the rotational degree of freedom of a *linear* molecule or

$$S_{\text{rot}} = 11.5 + \frac{R}{2} \ln\left(\frac{I_x I_y I_z}{\sigma}\right) + \frac{3}{2} \ln\left(\frac{T}{298}\right) \tag{38}$$

for the contribution of the rotational degrees of freedom for *non-linear* molecules and

$$S_{\text{vib}} = R \sum_\alpha \frac{\frac{h\nu_\alpha}{kT}\, \mathrm{e}^{h\nu_\alpha/kT}}{1 - \mathrm{e}^{h\nu_\alpha/kT}} - R \sum_\alpha \ln\left(1 - \mathrm{e}^{h\nu_\alpha/kT}\right) \tag{39}$$

for the vibrational degrees of freedom (see e.g. Benson 1976). M is the mass in atomic mass units and I_x, I_y and I_z are the principal moments of inertia in atomic units (AMU·Å^2). σ is the symmetry number of the cluster. The entropy in these equations is in units cal/K.

The contribution of the vibrational degrees of freedom to the entropy S is of the order of R (Benson 1976). This is much smaller than the translational and rotational contributions and, therefore, is neglected. Any contribution of excited electronic states to S can be neglected since such states in small molecules usually have excitation energys above 1 eV and, thus, are not populated at temperatures of the order of 1 000 K or less, which are of interest for circumstellar shells.

From the data given in Tab. 4 and the equations (34), . . . , (38) we can calculate the equilibrium abundance of a cluster of size N from the law of mass action

$$p_N = p_1^N \cdot \mathrm{e}^{-(\Delta H_f(N) - T\Delta S)/RT} \,. \tag{40}$$

ΔS is the difference between the entropy of one cluster of size N and the entropy of N monomers, p_N the partial pressure of the N-cluster and p_1 the partial pressure of the monomers in the gas phase. With the units usually applied in thermochemistry (ΔH_f in kcal/mol, S in cal/K) and the numerical values in (36), (37) and (38) the pressure is in units of atm.

4.2. The cluster size spectrum

Using the results for the bond energy of the clusters, their moments of inertia the symmetry numbers and the vibrational frequencies we can calculate the abundance of the $(MgO)_N$ clusters in a state of thermodynamic equilibrium. The result for a representative H_2 density of $10^{10}\,\text{cm}^{-3}$ typical for the condensation zone of a circumstellar dust shell is shown for four different temperatures in Fig. 4. For the highest temperature $T = 1\,100$ K the abundance of the clusters of size $N > 1$ relative to the monomer first decreases with increasing cluster size N and, then, increases with increasing cluster size N. This behaviour follows from quite general principles (e.g. Gail and Sedlmayr 1988).

Application of the law of mass action to the heterogeneous equilibrium between the monomer and the solid yields

$$\frac{1}{p_{1,v}} = \mathrm{e}^{-(\Delta H_{f,s} - T\Delta S_s)/RT} \,, \tag{41}$$

where $\Delta H_{f,s}$ is the enthalpy of formation of the solid from the monomers and ΔS_s the corresponding entropy change. $p_{1,v}$ is the partial pressure of the monomers in equilibrium with the condensed phase. We define the supersaturation ratio S' as

$$S' = \frac{p_1}{p_{1,v}} \tag{42}$$

and obtain from (40)

$$p_N = \exp\left[N \cdot \ln S' - \frac{\Delta H_f(N) - N \cdot \Delta H_{f,s}}{RT} + \frac{S(N) - N \cdot S_s}{R}\right] . \tag{43}$$

$\Delta H_f(N) - N \cdot \Delta H_{f,s}$ is the difference in the bond energies of monomers between the cluster and the solid. This difference is positive since the bond energy of monomers in the solid is higher than in a cluster built from a finite number of monomers. This can clearly be seen from Tab. 4 or Fig. 1. This bond energy defect results from the reduced attractive interaction energy of monomers with their environment for particles close to the surface as compared to interior particles. In a small cluster, all particles are close to the surface while for the solid such particles form a completely negligible fraction of all particles. In principle, the bond energy defect is roughly proportional to the surface area of the cluster, which in turn for compact structures varies roughly as $N^{\frac{2}{3}}$ with the number N of monomers.

For small cluster sizes $|\Delta H_f(N) - N \cdot \Delta H_{f,s}|/RT$ is a big number since the energy defect for small clusters is of the order of 2 to 3 eV per particle (cf. Fig. 1) while RT for a temperature

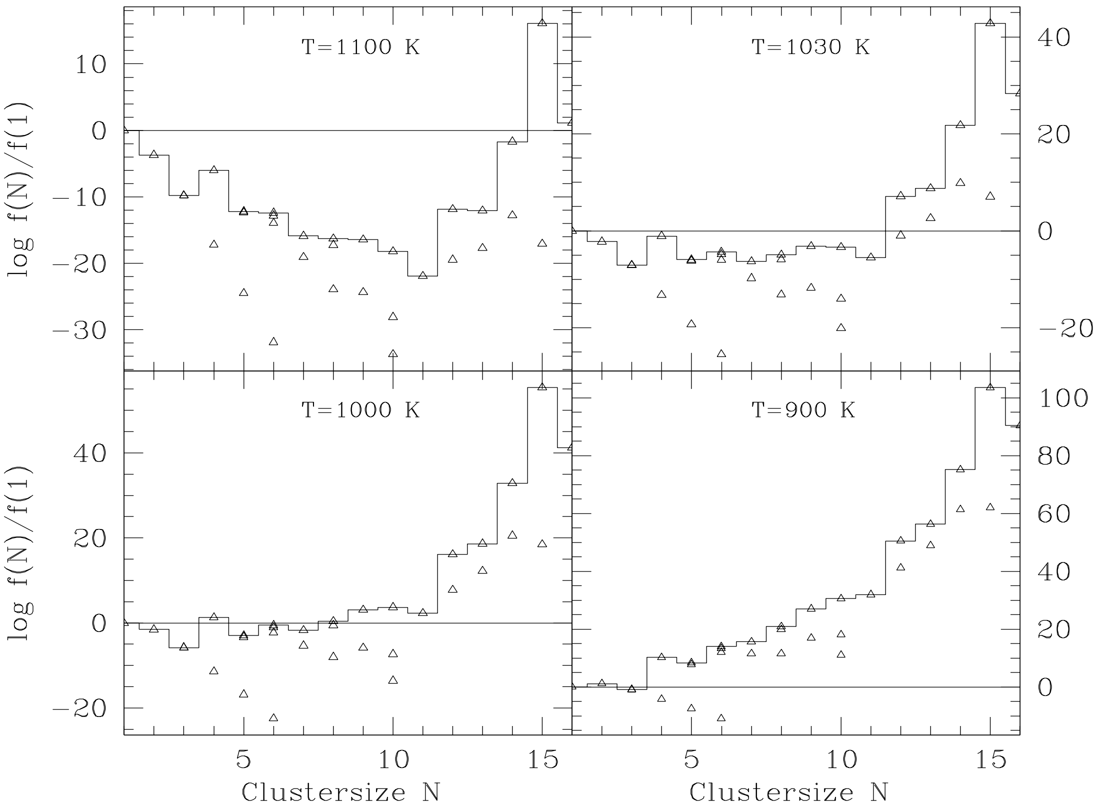

Fig. 4. Density of MgO clusters relative to the monomer density for different temperatures and a gas density of $n_{H_2} = 10^{10}\,\mathrm{cm}^{-3}$. The full line connects the most abundant clusters of each size. If this curve decreases for small cluster sizes and increases for large cluster sizes, nucleation occurs. In this case, the least abundant cluster on the curve defines the critical cluster for nucleation

of $\approx$ 1 000 K in the condensation zone of a circumstellar dust shell is of the order of 0.1 eV.

The entropy difference in (43) is dominated by the large and positive contribution of the translational degrees of freedom (cf. Eqs. (36), (37) and (38)), which shows only a weak logarithmic dependence on N. The contributions of the rotational and vibrational degrees of freedom are much smaller and the same holds for the entropy of the solid. The rotational contribution from the cluster shows only a weak logarithmic dependence on N. The entropy term, thus, can roughly be considered as constant.

The term $N \ln S'$ in (43) varies linearly with the cluster size N. It increases for a supersaturated vapour with $S' > 1$ and it decreases for a subsaturated vapour with $S' < 1$. We have to consider three different cases:

- $S' < 1$. All three terms in the exponential in Eq. (43) are negative. The equilibrium pressure of clusters relative to monomers decreases with increasing size N, though not necessarily in a monotonic way since there are strong individual scatterings in the bond energy between clusters of comparable size (cf. Fig. 1). The partial pressure of the clusters satisfies the following limit relation

$$\lim_{\substack{N\to\infty \\ S'<1}} p_N = 0\,. \tag{44}$$

- $S' > 1$. The term proportional to $\ln S'$ increases linearly with increasing N while the term describing the bond energy defect decreases proportional to $N^{\frac{2}{3}}$ with increasing N. If

$$\ln S' < \max_N \left| \frac{\Delta H_f(N) - N \cdot \Delta H_{f,s}}{RT} \right| \tag{45}$$

then the exponential in (43) first is dominated for small N by the big negative term proportional to the energy defect and, thus, p_N first decreases with increasing N. For sufficiently large N, however, the exponential becomes dominated by $N \ln S'$ and then p_N increases with N. For intermediate cluster sizes the size distribution p_N has a minimum for a certain value N_* of N. This behaviour can clearly be seen for instance in Fig. 4. Note, however, the strong individual scatterings between neighbouring N.
- $S' \gg 1$ and inequality (45) not satisfied. The exponential is always dominated by the term $N \ln S'$ and p_N only increases with increasing N, though not necessarily monotonicly. (The lowest temperature in Fig. 4 is close to this case.) The minimum N_* in the cluster size distribution here is taken for $N = 1$.

In any case, for a supersaturated vapour we have the following asymptotic behaviour of the equilibrium density of clusters for large N:

$$p_N \propto S'^N \quad \text{for} \quad S' > 1\ ,\ N \text{ large}\,. \tag{46}$$

5. Application to nucleation in stellar winds

5.1. Calculation of dust nucleation

The theoretical aspects of the dust formation and destruction processes are discussed in detail by Gail and Sedlmayr (1987). We restrict our considerations in this paper to the formation of MgO clusters and homogeneous particle growth, and neglect chemical sputtering and heteromolecular growth processes. In the general case of dust formation more than one growth species, like dimers and trimers, could be involved in the growth process. As we shall see, in our case the monomer can be adopted as the only growth species for MgO dust formation. Then the rate equations describing the nucleation process become much simpler. Our derivation of the nucleation rate given below is a simplified version adapted to the case of MgO nucleation of the more general discussion given in Gail and Sedlmayr (1988).

The net rate of change of the number density $f(N,t)$ of clusters of size N is the sum over the rates of all possible gain and loss processes of the N-cluster and is described by the master equation for the time evolution of $f(N,t)$

$$\frac{\mathrm{d}f(N,t)}{\mathrm{d}t} = R_\uparrow(N) - R_\downarrow(N) + R^\downarrow(N) - R^\uparrow(N) \tag{47}$$

where $R_\uparrow(N)$, $R_\downarrow(N)$ are the gain and loss rates from clusters of size $N-1$ to clusters of size N and vice-versa, and $R^\downarrow(N)$, $R^\uparrow(N)$ the corresponding gain and loss rates from $N+1$ to N. These rates are given by

$$R_\uparrow(N) = f(1,t)\,v_{N-1}\alpha_{N-1}\,A_{N-1}\,f(N-1,t) \tag{48}$$
$$R_\downarrow(N) = \beta_N\,A_N\,f(N,t) \tag{49}$$
$$R^\uparrow(N) = f(1,t)\,v_N\alpha_N\,A_N\,f(N,t) \tag{50}$$
$$R^\downarrow(N) = \beta_{N+1}\,A_{N+1}\,f(N+1,t) \tag{51}$$

where v_N is the root mean square thermal velocity

$$v_N = \sqrt{\frac{2kT}{\mu}} \quad \text{with} \quad \frac{1}{\mu} = \frac{1}{m_1} + \frac{1}{m_N} \tag{52}$$

of the monomers impinging onto the surface of an N-cluster, A_N the surface area of the N-cluster and α the sticking coefficient for monomers in collisions with an N-cluster. β_N is the vapourization rate per unit area of the surface. This rate can be determined from the principle of detailed balance between the growth process and its inverse process in a thermodynamic equilibrium state. In this state the growth and evaporation processes are in mutual equilibrium which requires

$$f(1)\,v_{N-1}\alpha_{N-1}\,A_{N-1}\,\overset{o}{f}(N-1) = \beta_N\,\overset{o}{f}(N)\,. \tag{53}$$

$\overset{o}{f}(N)$ is the density of N-clusters in equilibrium with the monomers in a thermodynamic equilibrium state. Eq. (53) defines β_N in terms of α_{N-1} and equilibrium densities. This Milne relation for β_N can be applied also in non-TE situations provided that the internal states of the N-cluster are populated thermally with some excitation temperature $T_d(N)$, which in circumstellar shells is likely to be different from the gas kinetic temperature T_g (e.g. Nuth and Donn 1981). We neglect here any non-TE level-population effects.

We define an effective transition rate

$$J_N(T) = f(1,t)\,v_{N-1}\alpha_{N-1}\,A_{N-1}\,\overset{o}{f}(N-1)\,\cdot \left[\frac{f(N-1,t)}{\overset{o}{f}(N-1)} - \frac{f(N,t)}{\overset{o}{f}(N)}\right]. \tag{54}$$

In terms of the effective transition rates J_N the master equations (47) can be written as

$$\frac{\mathrm{d}f(N,t)}{\mathrm{d}t} = J_N - J_{N+1}\,. \tag{55}$$

Next we define the total density of dust grains by

$$K_0(t) = \sum_{N=2}^{\infty} f(N,t)\,. \tag{56}$$

From (55) we obtain by summing the equations with $N \geq 2$

$$\frac{\mathrm{d}K_0(t)}{\mathrm{d}t} = J_2(t) \tag{57}$$

since there is no contribution from terms with $N \to \infty$ since arbitrarily big clusters cannot be formed. J_2 is the *nucleation rate* which we call J_*. As has been shown in Gail and Sedlmayr (1988) in a stellar wind with a sufficient mass-loss rate the densities $f(N,t)$ relax to a quasi-stationary equilibrium state for all N up to a certain $\hat{N}$. The effective transition rates J_N then are independent of N and equal to J_*. This means

$$J_* = \frac{f(N-1)}{\tau_{\mathrm{gr},N-1}} - \frac{f(N)}{\tau_{\mathrm{ev},N}} \tag{58}$$

with

$$\frac{1}{\tau_{\mathrm{gr},N}} = f(1)\,v_N\alpha_N\,A_N \tag{59}$$

$$\frac{1}{\tau_{\mathrm{ev},N}} = \frac{1}{\tau_{\mathrm{gr},N}}\,\frac{\overset{o}{f}(N-1)}{\overset{o}{f}(N)} \tag{60}$$

which denote the growth and evaporation rate, respectively. (58) is a system of equations for $f(N)$ and J_* in a quasi-stationary state. It holds for all N with $2 \leq N \leq \hat{N}$. It can be solved by eliminating successively $f(2), f(3), f(4), \ldots$ between consecutive equations (58) for $N = 2, \ldots, N = \hat{N}$. The result is (Gail and Sedlmayr 1988)

$$J_* \sum_{i=1}^{N} \frac{\tau_{\mathrm{gr},i}}{\overset{o}{f}(i)} = 1 - \frac{f(N+1)}{\overset{o}{f}(N+1)} \tag{61}$$

We draw two conclusions from this:

– $S' < 1$: As is discussed in sec. 4.2, for $S' < 1$ the size distribution $\overset{o}{f}$ satisfies the limit relation (44). The physically plausible solution in this case is

$$J_* = 0 \quad \text{and} \quad f(N) = \overset{o}{f}(N) \quad \text{for} \quad S' < 1\,. \tag{62}$$

Then, in the stationary case, the actual size distribution $f(N)$ equals the size distribution in the thermodynamic equilibrium state.

– $S' > 1$: For sufficiently large N, $\overset{o}{f}(N)$ is given by (46). This means

$$\lim_{\substack{N\to\infty \\ S'>1}} \overset{o}{f}(N) = \infty\,. \tag{63}$$

Since there cannot exist arbitrarily large clusters, $f(N)$ has to vanish above some (possibly very large) $N_{\max}$ and the second term on the r.h.s. of (61) then goes to zero for sufficiently large N. The nucleation rate J_*, then, is given by

$$J_* = \left[\sum_{i=1}^{N_{\max}} \frac{\tau_{\mathrm{gr},i}}{\overset{o}{f}(i)}\right]^{-1}\,. \tag{64}$$

Usually, $\overset{o}{f}(N)$ for $S' > 1$ has a sharp minimum in the sense that the smallest value of $\overset{o}{f}(N)$ taken at some N_* is much smaller than the value of $\overset{o}{f}(N)$ for any other N. This can clearly be seen, for instance, in Fig. (4). The sum in (64) then is determined by its biggest term $\tau_{\mathrm{gr},N_*}/\overset{o}{f}(N_*)$ [2]. The contribution of all other clusters of size $N \neq N_*$ can usually be neglected. Then the nucleation rate is given by

$$J_* = \frac{\overset{o}{f}(N_*)}{\tau_{\mathrm{gr},N_*}}\,. \tag{65}$$

Thus we have the very plausible result that the rate of dust particle formation is determined by the slowest growth step on the reaction chain along clusters of increasing size which occurs at the cluster size N_* where $\overset{o}{f}(N)$ is smallest.

(Note, however, that there exists a different possibility: If the least stable cluster with size N has an extremely low abundance compared to the cluster with size $N-1$ it is possible that the growth step from $N-1$ to $N+1$ by dimer addition becomes more efficient than the growth step from N to $N+1$ by monomer addition. Than the step from $N-1$ to $N+1$ becomes the rate determining step.)

Using (64) in (61) we obtain for the size distribution in the stationary case

$$f(N) = \overset{o}{f}(N)\,\frac{\sum\limits_{i=N}^{N_{\max}} \frac{\tau_{\mathrm{gr},i}}{\overset{o}{f}(i)}}{\sum\limits_{i=1}^{N_{\max}} \frac{\tau_{\mathrm{gr},i}}{\overset{o}{f}(i)}}\,. \tag{66}$$

[2] Note that this usually corresponds to the smallest $\overset{o}{f}(N)$, i.e. to $\overset{o}{f}(N_*)$, except if $\tau_{\mathrm{gr,N}}$ is very small just at this size for some special reason

For $N \leq N_*$ both sums can be approximated by the term with $N = N_*$. This shows

$$f(N) \approx \overset{o}{f}(N) \quad \text{for} \quad N < N_*\,,\ S' > 1\,, \tag{67}$$

i.e. in the subcritical region $N < N_*$ the size distribution equals the thermodynamic equilibrium size distribution. In this cluster size regime the relaxation time of the size distribution towards equilibrium is shorter than the slow changes of the total number of clusters with size $N < N_*$ introduced by the leakage at $N = N_*$ from subcritical clusters to the realm of dust grains with $N > N_*$.

For $N > N_*$ the sum in the denominator can be replaced by the term with $i = N_*$. In the nominator, the equilibrium size distribution $\overset{o}{f}(i)$ is increasing with increasing i for $i > N_*$ and for sufficient S' (cf. Eq. (46)) and small N the sum can be replaced by the single term with $i = N$. Then

$$f(N) = \frac{\tau_{\mathrm{gr},N}}{\tau_{\mathrm{gr},N_*}}\,\frac{\overset{o}{f}(N_*)}{\overset{o}{f}(N)} \tag{68}$$

This is the size distribution in a stationary equilibrium state which, however, is not realized for arbitrarily large cluster sizes $N \gg N_*$ (see Gail and Sedlmayr 1988).

5.2. Application to MgO dust formation in stellar winds

We are now prepared to determine the nucleation rate of MgO in circumstellar shells of M-stars. Figure 5 shows for a typical hydrogen density $n_{\mathrm{H}_2} = 10^{10}\,\mathrm{cm}^{-3}$ within the condensation zone of a circumstellar dust shell the cluster densities of $(\mathrm{MgO})_N$ clusters in the temperature range between 500 and 1500 K where circumstellar condensation is likely to occur. The partial pressure of MgO in the gas phase is calculated from chemical equilibrium in the gas phase considering the most abundant molecular species and the abundance of the $(\mathrm{MgO})_N$ clusters is calculated from (40). The critical cluster for nucleation according to our results obtained in the preceding section is that one for which the equilibrium density $\overset{o}{f}(N)$ is smallest for a given density and temperature. The size N_* of the critical cluster and its particle density then can be determined from the *lower envelope* of the family of curves $\overset{o}{f}(N)$ which is shown in Fig. 5. We read off from the Fig. that the critcal cluster size above ≈ 850 K is $N_* = 7$, between ≈ 650 and 850 K is $N_* = 3$ and below ≈ 650 K the critical cluster is the monomer $N_* = 1$ itself. The nucleation rate then can easily be calculated from Eq. (65).

The particle densities of the critical cluster are extremely small and make nucleation of MgO in circumstellar dust shells around M-stars as a dust species of its own or as seed nuclei for a different dust component completely impossible. At 850 K for instance we have a typical cluster density of the critical cluster of $\approx 10^{-17}\,\mathrm{cm}^{-3}$ and a typical collision frequency of the critical cluster with MgO molecules of

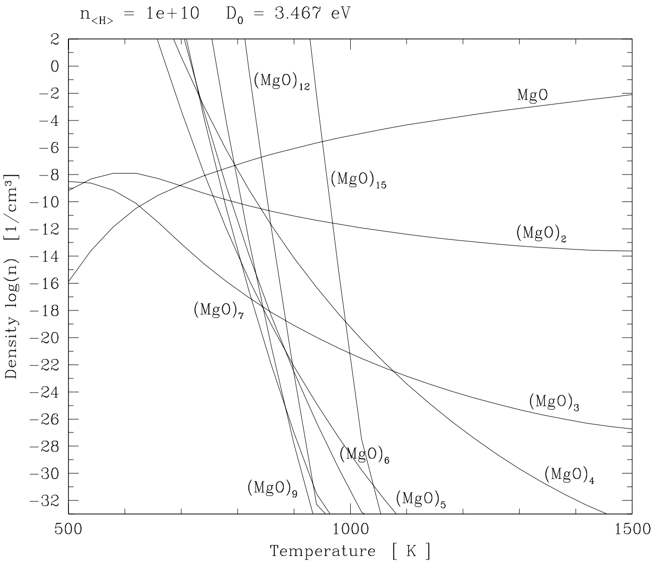

Fig. 5. Clusters in chemical equilibrium with the monomer at a hydrogen density of $n_{H_2} = 10^{10}\,cm^{-3}$ which is typical for the condensation zone. Shown are the densities for clusters of size $N = 1, \ldots, N = 15$

$\tau^{-1} = nv\sigma \approx 10^{-7} \cdot 10^5 \cdot 10^{-15} \approx 10^{-17}\,s^{-1}$. With a typical width of the condensation zone at the inner edge of the dust shell of $0.1\,R_* \approx 10^{13}$ cm and an expansion velocity of $\approx 2 \cdot 10^5\,cm{\cdot}s^{-1}$ near the sonic point the gas typically requires one year to cross the condensation zone of a circumstellar dust shell. Then we would obtain roughly 10^{-37} dust grains per hydrogen molecule. A lower condensation temperature of 650 K will increase this number to only 10^{-34} grains per hydrogen molecule while real dust shells contain roughly 10^{-13} dust grains per hydrogen nucleus. MgO nucleation, thus, is completely negligible, even as a subordinate dust component.

This does not result from a principal inability of MgO to form clusters but from the low bond energy of the MgO molecule, which according to recent determinations is only 3.5 eV (and, perhaps may be even lower, cf. sect. 2.4). The high abundance of hydrogen relative to both magnesium and oxygen on the one hand and the somewhat higher bond energy of 4.4 eV of the OH bond on the other hand makes it much more favorable for the oxygen atom to form an OH bond instead of a bond with Mg. Magnesium remains in this case in the gas phase mainly as the free Mg atom. The situation would be quite different if the bond energy of MgO were only slightly higher, as older determinations of the dissociation energy of MgO (≈ 4.1 eV) suggested, since then the formation of MgO would become more favourable and the resulting much higher gas phase abundance of MgO would result in efficient MgO nucleation (Gail and Sedlmayr 1986). Unfortunately, the precise nucleation rate depends critically on the uncertain value of the bond energy of MgO and a more definite conclusion with respect to the possibility or impossibility of MgO nucleation can only be drawn when a definitive value for the bond energy becomes available. Also, a less H-rich environment would increase the MgO abundance and MgO nucleation could then become an efficient process.

Finally it should be noted that the present calculation assumes equal numbers of Mg and O atoms in a cluster. In principle it is possible that non-stoichiometric clusters form by adding the more abundant Mg atoms to a cluster. Such clusters may exist in nature and addition of the abundant Mg and reactions with OH may significantly increase the growth rate and abundance of MgO clusters, but such clusters cannot be treated by the present potential model.

6. Concluding Remarks

We have discussed the process of nucleation of MgO in circumstellar dust shells. This discussion uses cluster properties which are calculated from a new semi-empirical potential model for II-VI compounds which is an extension of the standard semi-empirical potential (e.g. Martin 1983) used in the discussion of pure ionic clusters of I-VII compounds (alkali-halides). The new potential model accounts for the partially ionic, partially covalent bond character of alkaline-earth chalcogenides like MgO. It is shown that such a potential model can be applied to model simultaneously the properties of the molecule and that of the solid and can be applied to calculate the structure and properties of clusters of all intermediate sizes N.

The method applied in this paper to calculate nucleation rates is free from the arbitrary and unrealistic assumptions on which discussions of dust nucleation in circumstellar shells have been based up to now, especially when compared to classical homogeneous nucleation theory (cf. Sedlmayr 1994) used to calculate nucleation rates as is presently done. This has always been a subject of strong criticism (e.g. Nuth and Donn 1985).

This paper presents for the first time a method by which such calculations can be put on much safer basis. It can be extended to other compounds which are perhaps more likely to be responsible for nucleation in M-stars. This requires that similar semi-empirical potential models are constructed for compounds like $(SiO)_N$, Al_NO_M or mixed oxide clusters of Si, Mg, Fe etc. which in principle is not too difficult. An extension of the calculations presented in this paper to the case of the nucleation of the MgS dust observed in C-Stars is possible and the results will be presented in a separate paper (Köhler et al. 1996).

Acknowledgements. We thank the referee J.A. Nuth for carefully reading the manuscript and his suggestions for improving the presentation. This work has been supported by the Deutsche Forschungsgemeinschaft (DFG), Schwerpunktprogramm *Theorie kosmischer Plasmen*, project Ga 162/2, Ga 162/3.

References

Bauschlicher Jr. C.W., Lengsfield III B.H., Liu B., 1982, J. Chem. Phys. 77, 4084
Bauschlicher Jr. C.W., Partridge H., 1993, Chem. Phys. Lett. 205, 497
Begemann B., Dorschner J., Henning T., Mutschke H., Thamm E., 1994, ApJ 423, L71

Benson S.W., 1976, Thermochemical Kinetics, Wiley & Sons, New York
Berkowitz J., 1958, J. Chem. Phys. 29,1386
Berkowitz J., 1958, J. Chem. Phys. 29,1386
Born M., Mayer, J.E., 1932, Zeitschr. f. Phys. 75, 1
Boswarva I.M., 1970, Phys. Rev. B 1, 1698
Bramscomb L.M., 1962, in Atomic and Molecular Processes, D.R. Bates Ed., Academic Press, New York, p. 100
Brumer P., Karplus M., 1973, J. Chem. Phys. 58, 3903
Causa M., Dovesi R., Pisani C., Roetti C., 1986, Surf Sci. 175, 551
Chase Jr. M.W., Davies C.A., Downey Jr. J.R., Frurip D.J., McDonald R.A., Syverud A.N., 1985, JANAF Thermochemical Tables, J. Phys. Chem. Ref. Data 14, Suppl 1, National Bureau of Standards (US)
Cuesta I.G., de Meras A.S., Gil I.N., 1991, Chem. Phys. Lett. 186, 386
Cuesta I.G., de Meras A.S., Gil I.N., 1991, Chem. Phys. Lett. 205, 484
Donn, B., Nuth, J.A., 1985, ApJ 288, 187
Forrest W.J., Houck J.R., McCarthy J.F., 1981, ApJ 248, 195
Fowler P.W., Madden P.A., 1985, J. Phys. Chem. 89, 2581
Gail H.-P., Sedlmayr E., 1986, A&A 166, 225
Gail H.-P., Sedlmayr E., 1987, in Physical Processes in Interstellar Clouds, eds. G. Morfill and M. Scholer, Reidel, Dordrecht, p. 275
Gail H.-P., Sedlmayr E., 1988, A&A 206, 153
Goebel J.H., Moseley S.H., 1985, ApJ 290, L35
Henning T., Begemann B., Mutschke H., Dorschner J., 1995, A&AS 112, 143
Hirschfelder J.O., Curtiss C.F., Bird R.B., 1964, Molecular theory of gases and liquids, 2nd printing, John Wiley & Sons, New York
Huber K.P., Herzberg G., 1979, Molecular Spectra and Molecular Structure Vol 4, Van Nostrand Reihold
Huggins M.L., Sakkamoto Y., 1957, J. Phys. Soc. Japan 12, 241
Iben Jr., I., 1991, Single and binary star evolution, *Astrophysical Journal Supplement* 76, 55-114
Köhler T.M., 1988, Anwendung der Evolutionsstrategie auf die Berechnung der Gleichgewichtskonfigurationen von MgS-Clustern, Studienarbeit, Technical University Berlin
Köhler T.M., 1989, Gleichgewichtskonfigurationen astrophysikalisch relevanter kleiner anorganischer Cluster, Diploma thesis, Technical University Berlin
Köhler T.M., Gail H.-P., Sedlmayr E., 1996, (*in preparation*)
Landolt-Börnstein, 1981, Zahlenwerte und Funktionen, Springer, Berlin
Martin T.P., 1983, Phys. Rep. 95, 167
Nuth J.A., Donn B., 1981, ApJ 247, 925
Nuth J.A., Moseley H., Silverberg R.F., Goebel J.H., Moore W.J., 1985, ApJ 290, L41
Nuth J.A., Hecht J.H., 1995, Ap&SS 163, 79
O'Konski C.T., 1955, J. Chem. Phys. 23, 1174
O'Konski C.T., Higuchi W.I., 1955, J. Chem. Phys. 23, 1175
Omont A., Moseley S.H., Cox P., Glaccum W., Casey S., Forveille T., King-Wing Chan, Sczerba R., Loewenstein R.F., Harvey P.M., Kwok S., 1995, ApJ 454, 819
Operti L., Tews E.C., MacMahon T.J., Freiser B.S., 1989, J. Am. Chem. Soc. 111, 9152
Patzer A.B.C., Köhler T.M., Sedlmayr E., 1995, Planetary and Space Sci. 43, 1233
Pauling L., 1960, The Nature of the Chemical Bond and the Structure of Molecules and Crystals, 3rd Ed., Cornell University Press
Pedley J.B., Marshall E.M., 1983, J. Phys. Chem. Ref. Data 12, 967
Rechenberg I., Evolutionsstrategie – Optimierung technischer Systeme nach Prinzipien biologischer Evolution, frommann-holzboog, Stuttgart
Rechenberg I., 1989, in Machine Learning: Principles and Techniques, ed. R. Forsyth , Chapman and Hall, London, p. 83
Recio J.M., Pandey R., Ayuela A., Kunz A.B., 1993, J. Chem. Phys. 98, 4783
Rittner E.S., 1951, J. Chem Phys. 19, 1030
Saunders W.A., 1988, Phys. Rev. B 37, 6583
Saunders W.A., 1989, Z. Phys. D 12, 601
Sedlmayr E., 1994, in Molecules in the Stellar Environment, ed. U.G. Jørgensen, Springer, Berlin, p. 163
Sumino Y., Anderson O.L., Suzuki I., 1983, Phys. Chem. Minerals 9, 38
Tessma J.R., Kahn A.H., Shockley W., 1953, Phys. Rev. 92, 890
Unsöld A., 1927, Zeitschr. f. Phys. 43, 563
Weast R.C., Astle M.J., Beyer W.H., 1988, CRC Handbook of Chemistry and Physics, 69th Ed., CRC press, Boca Raton
Ziemann P.J., Castleman A.W., 1991, J. Chem Phys. 94, 718

A. Calculation of the structure and bond energy of clusters

The stable equilibrium configuration of a cluster with N atoms is determined by the local minima of the potential $\Phi(q_{i\mu})$ in the $3N$-dimensional space of the positions $q_{i\mu}$ of its individual atoms ($i = 1, \ldots, N$ labels the atoms, $\mu = 1, 2, 3$ their cartesian coordinates). The ground state of the cluster corresponds to the absolute minimum of the potential. The basic problem then is to determine the absolute minimum of the cluster potential $\Phi(q_{i\mu})$ and all other deep local potential minima with comparable depth to that of the ground state.

As is well known, such an optimization problem with a large number of variables cannot be solved directly by analytical methods and the task of solving the problem by numerical methods becomes extremely difficult and time consuming if the surfaces $\Phi(q_{i\mu}) = const$ have a complicated geometric structure. Up to now, no general method is known which allows one

1. to find definitely *all* local extrema of an optimization problem and
2. to decide whether the real optimum is contained within the set of extrema found by the applied method.

Numerous methods, however, have been developed which allow one to find in a certain sense a best result, which means that for test cases with a known absolute minimum the algorithm always finds this minimum or at least a local minimum not much different from the absolute one.

One method, which has been applied in the past successfully to several difficult optimization problems like that of the travelling salesman is the "evolution strategy" developed by Rechenberg (1973, 1989). We apply this method to determine the possible equilibrium configurations of ionic clusters.

The special variant of the method used in our computation is the (1,10)-evolution strategy (Rechenberg 1973, 1989), which proceeds in the following manner: Starting from an initial vector $\boldsymbol{O}_p$ in the variable space (called *parent*) and an initial step length δ_p, ten new vectors $\boldsymbol{O}_{\mathrm{off},j}$ ($j = 1, \ldots, 10$), called *offsprings*,

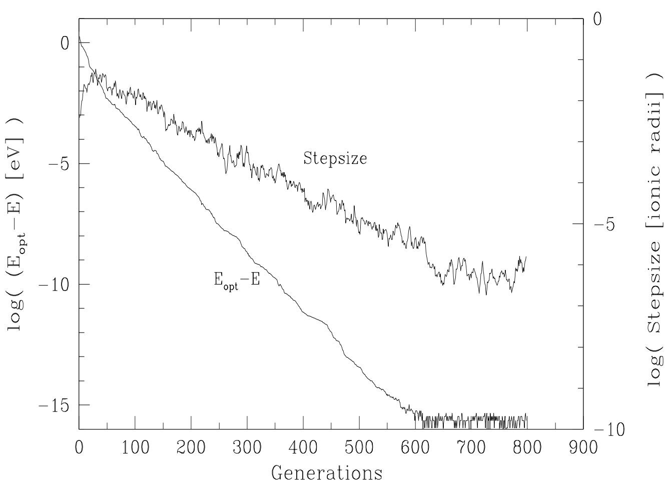

Fig. 6. Example for the minimum search of the cluster potential for the N = 4 MgO cluster using the evolution strategy. The difference $E_{\rm opt} - E$ (left scale) is the energy difference between some cluster configuration tried during the otimising process and its final value. The nearly horizontal part after 600 generations is due to the machine accuracy. The stepsize (right scale) are the steplengths $\delta_{\rm off}$ in units of the ionic radii.

are generated by adding to the parent $\boldsymbol{O}_p$ new vectors $\delta_{{\rm off},j} \cdot \boldsymbol{z}_i$. The vectors $\boldsymbol{z}_i$ are unit vectors with components which are normally distributed random numbers with variance $\sigma = 1/\sqrt{6N}$. The numbers $\delta_{{\rm off},j}$ are the individual step length's, generated from δ_p by multiplying this by logarithmic normally distributed random numbers $\xi_j = k^{y_j}$ with $k > 1$ where the y_j are normally distributed such that the numbers δ_p/ξ_j and $\delta_p\xi_j$ are distributed with the same probability. k determines the width of the distribution of step length's. Numerical experience shows $k = 1.5$ to be a reasonable choice for most problems (Rechenberg 1973).

The best offspring, i.e. that offspring whose quality function $Q(\boldsymbol{O}_{\rm off})$ is nearest to the optimum, is declared as the new parent of the next generation and its step length $\delta_{{\rm off},j}$ is declared as the new step length δ_p of the next generation. In our case the quality function is the cluster potential and the best offspring is that which results in the lowest potential energy.

The basic idea of the whole method is to approach the optimum by an intelligent trial and error strategy, in which the experience with respect to the optimum step sizes is left from generation to generation in the "evolution" process. Since the step length itself is varied by a random process, from time to time "mutations" of the step lengths occur if a big side-step improves the quality. This prevents the process from being trapped into a deep local isolated minimum. Its numerical efficiency stems from the fact that only the quality function has to be evaluated a few times in each generation. Its derivatives are *not* required and the method is well suited for treating even unpleasant quality functions, even those with discontinuities.

The search for the absolute minimum is stopped if the step lengths drops below some prescribed (small) limit because this indicates that further "mutations" do not improve the result (cf. Fig. 6 for an example). All local deep minima encountered during the search are stored because these are required for determining the isomers. Details with respect to the application of the evolution strategy to the calculation of cluster structures are described in Köhler (1988, 1989).

This article was processed by the author using Springer-Verlag LaTeX A&A style file *L-AA* version 3.